

Benzannelation Effect on Eneidyne Cycloaromatization: An ab Initio Molecular Orbital Study

Shiro Koseki*

Chemistry Department for Materials, Faculty of Engineering, Mie University, Tsu 514-0008, Japan

Yuichi Fujimura and Masahiro Hiramata

Department of Chemistry, Graduate School of Science, Tohoku University, Sendai 980-8578, Japan

Received: April 2, 1999; In Final Form: July 22, 1999

The mechanism of altering the rate-limiting step in eneidyne cycloaromatization (Bergman reaction) by benzannelation has been studied using ab initio molecular orbital (MO) methods. The calculated results indicate that the benzannelation effect cannot be interpreted by the energy separation between the lowest singlet and triplet states in *p*-benzyne-type intermediates **2** and **4**, as revealed for *p*-benzyne **6** and 1,4-diylnaphthalene **7**. The energy barriers for the retro-cyclizations of the intermediates to produce cyclodec-3-ene-1,5-diyne (**1**) and 3,4-benzo-cyclodec-3-ene-1,5-diyne (**3**) are estimated to be 15.3 and 5.9 kcal/mol, respectively. Hydrogen abstractions from methane by *p*-benzyne-type intermediates in the Bergman reaction of **1** and **3** are calculated to have energy barriers of 12.7 and 11.8 kcal/mol. From these theoretical results on the energy barriers of retro-cyclizations and hydrogen abstraction, we concluded that the rate-limiting step in Bergman reaction of **3** is hydrogen abstraction rather than cyclization, while that of **1** is cyclization.

1. Introduction

In recent years, the mechanisms of Bergman cyclization have attracted considerable attention because of the possibility that *p*-benzyne-type intermediates are the intermediates in the biological activity of the eneidyne family of antitumor antibiotics.^{1–7} Bergman cyclization consists of cyclization and hydrogen abstractions. It is widely known that the rate-limiting step in the Bergman cyclization of acyclic eneidyne system is cyclization, independent of the solvent reagents used as hydrogen donors. However, recent studies^{8,9} indicate that hydrogen abstraction is a rate-limiting step in Bergman reaction of 10-membered benzenediyne (**3** in Figure 1). This difference in the rate-limiting step between acyclic and aromatic ring condensed systems was thought to be due to a ring strain effect and/or a benzannelation effect.

Quite recently, Kaneko et al.⁹ confirmed that cyclization is the rate-limiting step in the reaction of a 10-membered eneidyne (**1**) with no benzene ring. Furthermore, they demonstrated that benzannelation to the even acyclic eneidyne alters the rate-limiting step in Bergman cyclizations. Kaneko et al.⁹ proposed two possible mechanisms for altering the rate-limiting step by benzannelation: (1) a faster rate of retro-Bergman cyclization and (2) a slower rate of hydrogen abstraction by the aromatic ring condensed 1,4-dihydrobenzene intermediate. The first mechanism is qualitatively justified by noting the change in aromaticity of **2** and **4** during retro-Bergman cyclization; i.e., **4** shows a partial loss of resonance energy while **2** shows a full loss. The second mechanism was based on the assumption that benzannelation would induce a substantial singlet–triplet energy splitting. This may cause a slower rate of hydrogen abstraction, i.e., the rate-limiting step, in the singlet ground state of **4**.

To investigate which mechanism is responsible for altering the rate-limiting step, we performed an ab initio molecular orbital (MO) study. We estimated the effect of benzannelation

on the singlet–triplet energy separation in **2** and **4**, as well as *p*-benzyne (**6**) and 1,4-diylnaphthalene (**7**). We also investigated the effect of benzannelation on the energy profile of the Bergman reactions, **1** → **2** and **3** → **4**. Our theoretical study reveals that it is the faster rate of the retro-Bergman cyclization that is responsible for altering the rate-limiting step.

2. Methods of Calculation

Full-optimized reaction space multiconfiguration self-consistent field (FORSCSCF, equivalent to CASSCF¹⁰) methods with 6-31G(d,p)¹¹ and TZV(d,p)¹² basis sets were employed in order to optimize the geometries of *p*-benzyne-type intermediates. The MCSCF active space included all occupied π orbitals and the inner set of virtual π orbitals as well as two radical σ orbitals; i.e., there are eight electrons in 8 active orbitals for *p*-benzyne **6** (Figure 2) and 12 electrons in 12 active orbitals for 1,4-diylnaphthalene **7**. In the following discussion, these methods are referred to as MCSCF(8,8) and MCSCF(12,12), respectively. The numbers of configuration state functions included in these MCSCF calculations are 264 (a_g symmetry) and 300 (b_{3u} symmetry) for **6**, and 58 016 (a_1 symmetry) and 96 192 (b_1 symmetry) for **7**. The relative energies of the geometrical structures were re-estimated using the MCSCF method followed by second-order Moller–Plesset perturbation calculations.¹³ This method is referred to as MCSCF+MP2.

A smaller MCSCF active space was employed with the 6-31G(d,p) basis set in the study of the reactions **1** → **2** → **5** and **3** → **4**, because of the limitation of our computer systems. The space included two radical σ orbitals, three π and three π^* orbitals, and the σ and σ^* orbitals of the C–C bond which is broken along the reaction path. This method is referred to as MCSCF(10,10)/6-31G(d,p).

All calculations were carried out using the quantum chemistry program code GAMESS.¹⁴

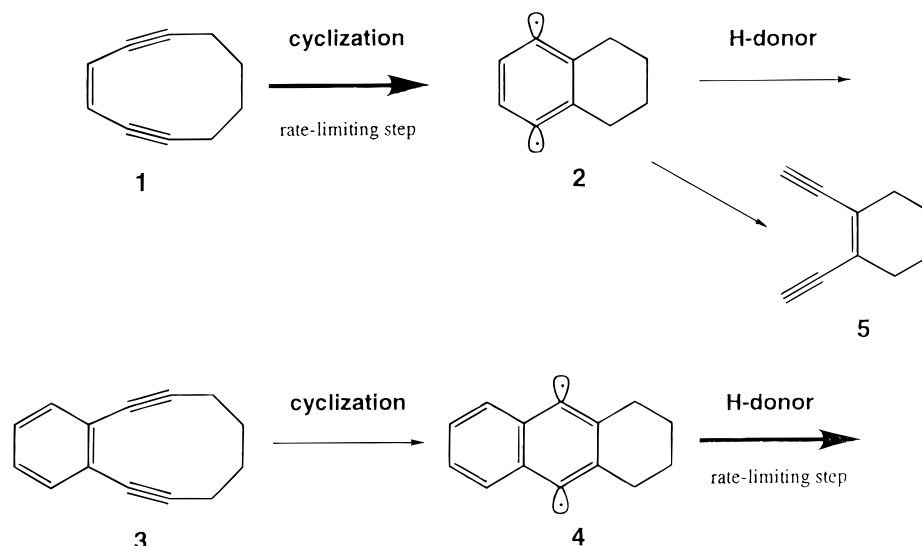


Figure 1. Rate-limiting step in Bergman cyclization of strained cyclic enediynes.

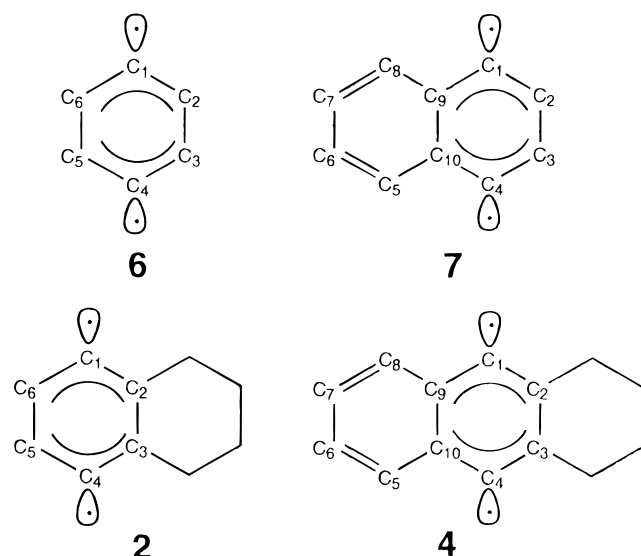


Figure 2. Atom numbers and bond alternation in *p*-benzyle (6), 1,4-diylnaphthalene (7), 2, and 4.

3. Results and Discussion

3.1. Singlet–Triplet Energy Separation ΔE_{ST} . Kaneko et al.⁹ assumed that benzannulation induces a substantial singlet–triplet splitting ΔE_{ST} on the basis of Chen's rationale;¹⁵ namely, larger ΔE_{ST} in a diradical intermediate may cause the intermediate to be a poor hydrogen abstraction agent. Therefore, we first have examined ΔE_{ST} in the intermediates of interest.

Table 1 lists the singlet and triplet energies of two *p*-benzyl-type intermediates, 6 and 7, calculated at several levels of MO theory. The MCSCF calculations give 2.6–2.9 kcal/mol to ΔE_{ST} in 6, while ΔE_{ST} of 4.6–5.2 kcal/mol is obtained for 6 using the MCSCF+MP2 methods. These values are consistent with recent theoretical results.^{16–19} The experimental separation (3.8 \pm 0.5 kcal/mol as measured by photoelectron spectroscopy)²⁰ falls in the middle of the theoretical values. It seems that the MCSCF+MP2 method overestimates the difference in the dynamic correlation between the singlet and triplet states. Since ΔE_{ST} increased by only 0.1 kcal/mol after the expansion of the basis set from 6-31G(d,p) to TZV(d,p), it is unlikely that ΔE_{ST} would change greatly even if a better basis set was employed (Table 1). Similarly, zero-point energy (ZPE) correction obtained

TABLE 1: Energy Difference ΔE_{ST}^a [kcal/mol] between the Lowest Singlet and Triplet States Obtained at Various Levels of Theory

molecule	method	ΔE_{ST}	
<i>p</i> -benzyle (6)	MCSCF(8,8)/6-31G(d,p)	2.6	
	MCSCF(8,8)/6-31G(d,p) + ZPE ^b	2.8	
	MCSCF(8,8)/TZV(d,p)	2.7	
	MCSCF(8,8)/TZV(d,p) + ZPE ^b	2.9	
	MCSCF(8,8)+MP2/6-31G(d,p)	4.6	
	MCSCF(8,8)+MP2/6-31G(d,p) + ZPE ^b	4.8	
	MCSCF(8,8)+MP2/TZV(d,p)	5.0	
	MCSCF(8,8)+MP2/TZV(d,p) + ZPE ^b	5.2	
	CASSCF(8,8)/aANO ^c	3.8	
	CASPT2(8,8)/aANO ^c	5.8	
	CCCI/pVTZ/MCSCF(8,8)/3-21G ^c	2.3	
	CASMP2(6,6)/6-31G(d) ^d	2.1/0.7 ^e	
BLYP/6-311+G(d,p) ^f	1.5		
CASPT2(12,12)/cc-pVDZ+ZPE ^g	5.8		
expt ^h	3.8 \pm 0.5		
1,4-diylnaphthalene (7)	MCSCF(12,12)/6-31G(d,p)	2.5	
	MCSCF(12,12)/6-31G(d,p) + ZPE ^b	2.6	
	MCSCF(12,12)/TZV(d,p)	2.5	
	MCSCF(12,12)/TZV(d,p) + ZPE ^b	2.6	
	MCSCF(12,12)+MP2/6-31G(d,p)	5.0	
	MCSCF(12,12)+MP2/6-31G(d,p) + ZPE ^b	5.1	
	MCSCF(12,12)+MP2/TZV(d,p)	5.2	
	MCSCF(12,12)+MP2/TZV(d,p) + ZPE ^b	5.3	
	CASPT2(12,12)/cc-pVDZ+ZPE ^g	5.6	
	derived from isodesmic reactions ^g	5.4	
	2 (C ₂)	MCSCF(10,10)/6-31G(d,p)	2.8
	MCSCF(10,10)+MP2/6-31G(d,p)	4.4	
4 (C ₂)	MCSCF(10,10)/6-31G(d,p)	3.0	
MCSCF(10,10)+MP2/6-31G(d,p)	5.0		

^a $\Delta E_{ST} = E(^3B_{3u}/^3B_1) - E(^1A_g/^1A_1)$. ^b ZPE = zero-point energy. ZPE is estimated by using MCSCF(8,8)/6-31G(d,p). ^c Reference 16. ^d Reference 17. ^e Vertical/adiabatic excitation. See ref 17 for the details. ^f Reference 18. ^g Reference 19, the details are also given. ^h Reference 20.

at MCSCF levels of calculations would not make any significant contribution to ΔE_{ST} . This tendency is similar to that demonstrated in results reported previously.^{16–19}

ΔE_{ST} in 7 is calculated to be 2.5–2.6 kcal/mol at the MCSCF levels of theory. After the dynamic as well as the static correlation was taken into account using the MCSCF+MP2 method, ΔE_{ST} increased to 5.0–5.3 kcal/mol. This is essentially equal to Squires' results.¹⁹ That is, even though the MCSCF+MP2 method overestimates the difference in the dynamic correlation between the singlet and triplet states as discussed for 6, ΔE_{ST}

TABLE 2: Bond Lengths [Å]^a

molecule	bond	lowest singlet	lowest triplet
p-benzyne (6)	C ₁ –C ₂	1.3824 (1.3789)	1.3867 (1.3836)
	C ₂ –C ₃	1.4111 (1.4101)	1.4029 (1.4011)
1,4-diyl-naphthalene (7)	C ₁ –C ₂	1.3605 (1.3564)	1.3640 (1.3602)
	C ₁ –C ₉	1.4130 (1.4103)	1.4177 (1.4152)
	C ₂ –C ₃	1.4374 (1.4373)	1.4305 (1.4297)
	C ₉ –C ₁₀	1.4319 (1.4298)	1.4205 (1.4178)
	C ₁₀ –C ₅	1.4241 (1.4223)	1.4240 (1.4222)
	C ₆ –C ₇	1.4196 (1.4182)	1.4215 (1.4202)
2 (C ₂)	C ₅ –C ₆	1.3740 (1.3713)	1.3738 (1.3711)
	C ₁ –C ₂	1.3854	1.3927
	C ₁ –C ₆	1.3770	1.3795
4 (C ₂)	C ₂ –C ₃	1.4464	1.4300
	C ₅ –C ₆	1.4125	1.4068
	C ₁ –C ₂	1.3517	1.3573
	C ₁ –C ₉	1.4202	1.4246
	C ₂ –C ₃	1.4945	1.4765
	C ₉ –C ₁₀	1.4119	1.4017
	C ₁₀ –C ₅	1.4128	1.4132
	C ₆ –C ₇	1.3758	1.3754
	C ₅ –C ₆	1.3927	1.3947

^a The numbering of atoms is depicted in Figure 2. The bond lengths are in angstroms. The lengths are obtained using the 6-31G(d,p) basis set, while the TZV(d,p) basis set gives those in the parentheses, where MCSCF(8,8) was used for **6**, MCSCF(12,12) was used for **7**, and MCSCF(10,10) was used for **2** and **4**. The Cartesian coordinates of these structures are given in Table 1S (Supporting Information).

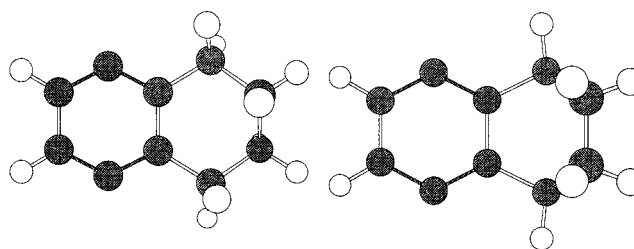
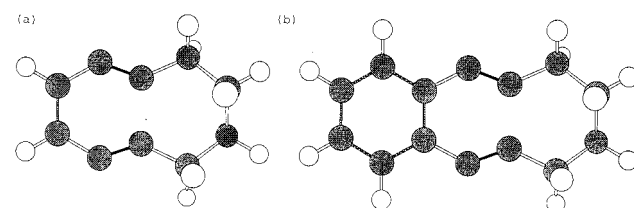
in **7** is quite similar to that in **6**. This indicates that there is no benzannelation effect on ΔE_{ST} in **7**. The main reason why this effect on ΔE_{ST} is observed is that the through-bond interaction occurs only among the radical (σ) orbitals and the C₂–C₃ (C₅–C₆ or C₉–C₁₀; σ) orbitals,²¹ and there is no direct interaction of these σ orbitals with the π orbitals of the adjacent aromatic ring of **7**.

We have also estimated ΔE_{ST} in **2** and **4**. Although the ΔE_{ST} values are somewhat smaller than those in **6** and **7**, there is essentially no difference in ΔE_{ST} between **2** and **4**. Namely, no benzannelation effect on ΔE_{ST} is observed in **4**.

3.2. Geometrical Structures. Table 2 lists the C–C bond lengths of **6** and **7** optimized at MCSCF/6-31G(d,p) and MCSCF/TZV(d,p) levels of theory.²² The corresponding C–C bond lengths in **2** and **4** are also cataloged in this table. The C–C bond lengths in these molecules are quite similar in both the singlet and triplet states, and **6** and the benzyne moieties of **7**, **2**, and **4** have an antiquinoid form (Figure 2). The C₁–C₂ bond in the singlet state of **7** is 0.022 Å shorter than that of **6**. On the other hand, the bond lengths of C₁–C₉ and C₂–C₃ are 0.031 and 0.026 Å longer than the corresponding bonds in **6**. However, these small differences in bond length do not produce any significant change in the through-bond interaction in **6** and **7**.

The above conclusion is also true for **2** and **4**. In addition, it is also worthy of note that the C₂–C₃ bond length in **2** and **4** is 0.035 and 0.057 Å longer than the corresponding bond lengths in **6** and **7**, respectively (Table 2).²² Since the C₂–C₃ bond is broken along the retro-cyclization path, we may predict that the energy barrier of retro-cyclization in **2** and **4** is explicitly lower than that in **6** and **7**. This prediction is verified below.

3.3. Reactions of Cyclization. Two energy minima (C₂ and C_s) were located for **2** and **4**, respectively, where Figure 3 illustrates the geometrical structures of **2**.²² The corresponding energy minima were also found for **1** and **3**. The C₂ symmetric structures for **2** and **4** are lower in energy than the corresponding C_s symmetric structures by 3.5 and 2.5 kcal/mol, respectively. The C₂ structures of **1** and **3** are also about 8 kcal/mol lower in

**Figure 3.** C₂ (left) and C_s (right) structures of **2**.**Figure 4.** Transition state structures optimized by the MCSCF(10,10)/6-31G(d,p) method: (a) TS (**1** → **2**) and (b) TS (**3** → **4**).**TABLE 3: Relative Energies [kcal/mol] of Stationary Geometries in Cyclization^a**

method	MCSCF(10,10)	MCSCF(10,10)+MP2 ^c	expt
1	–22.4	+1.8	
TS (1 → 2) ^b	+16.0	+15.3	refs 30, 31 ^d
2	0	0	
3	–33.7	–10.3	
TS (3 → 4) ^b	+9.2	+5.9	refs 30, 32 ^e
4	0	0	
TS (2 → 5) ^b	+17.5	+18.2	+9.5 ^f
5	–26.0	–3.8	

^a MCSCF(10,10)/6-31G(d,p). The C₂ structures are used. See the text. ^b TS indicates transition state. See ref 23. ^c MCSCF(10,10)/6-31G(d,p) geometries were employed. ^d The energy difference between **1** and TS (**1** → **2**) was estimated to be 24.4 (ref 30) or 23.8 (ref 31) kcal/mol. ^e The energy difference between **3** and TS (**3** → **4**) was estimated to be 25.0 kcal/mol (ref 30). ^f The energy difference has been observed for the hydrogen abstraction of **2** from methanol. See refs 15, 25, and 29.

energy than the corresponding C_s structures. These energy differences are caused by ring strain, which is demonstrated by the large C–C–C bond angles around methylene carbons, especially in **1** and **3**. Thus, since the C₂ structures are commonly more stable than the corresponding C_s structures, the C₂ reaction paths of **1** → **2** and **3** → **4** were investigated in this study.

Transition states were located along the C₂ paths of the cyclization reactions **1** → **2** and **3** → **4**.²³ The geometrical structures are depicted in Figure 4,²² and their relative energies are shown in Table 3. The C₂–C₃ distances (1.900 and 1.860 Å) at these transition states are somewhat shorter than that (1.993 Å) obtained in the retro-cyclization of **6**.²⁴ This is apparently attributable to the linkage by a methylene chain. On the other hand, the C₁–C₄ distances are quite similar to that in **6**.²⁴

The MCSCF results indicate that **1** was more stable than **2** by more than 20 kcal/mol, while the reverse order is obtained by MCSCF+MP2, even though the energy difference was small (1.8 kcal/mol). Schottelius et al. have reported the same result for 9,10-dehydroanthracene intermediate.²⁵ We attribute such a peculiar result to the fact that the effect of dynamic correlation in radical systems is estimated to be rather larger than that in a closed-shell system when perturbation methods such as the MCSCF+MP2 method are used. On the other hand, the energy barrier of the retro-cyclization (the energy difference between **2** and TS(**1** → **2**)) would not show the peculiar result because both **2** and TS(**1** → **2**) have comparable radical character.

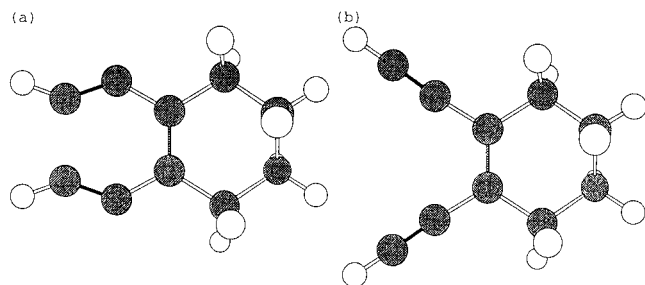


Figure 5. Geometrical structures of (a) transition state **TS** ($2 \rightarrow 5$) and (b) product **5** optimized by the MCSCF(10,10)/6-31G(d,p) method.

The energy barrier of the ring-opening reaction $2 \rightarrow 1$ is estimated to be 15.3 kcal/mol. This barrier is about 4 kcal/mol lower than that of the corresponding reaction in **6**.^{24,26}

The energy barrier of $4 \rightarrow 3$ is lower than that of $2 \rightarrow 1$ by about 9 kcal/mol, which is close to the corresponding experimental energy difference for **6** and **7**.²⁹ Rough estimation using the MCSCF(4,4) + MP2/6-31G(d,p) method²⁸ provides energy barriers of 12.7 and 11.8 kcal/mol for the hydrogen abstractions from methane by **2** and **4**, respectively. An MCSCF calculation with larger active space is expected to exhibit a lower energy barrier. These barrier heights are comparable with the results (9.5 kcal/mol) obtained by Logan et al.¹⁵ since they have employed methanol as a hydrogen donor.^{25,29} Thus, the energy barrier of hydrogen abstraction is estimated to be higher than that of $4 \rightarrow 3$ retro-cyclization so that hydrogen abstraction appears to be the rate-limiting step in the Bergman reaction of **3**; that is, benzannulation must reduce the energy barrier of retro-cyclization. The present ab initio calculations support the suggestions made by Kaneko et al.⁹

Kaneko et al.⁹ also suggested the alternative reaction path for the ring-opening reaction $2 \rightarrow 5$ (Figure 5). We have successfully located the transition state along this reaction path. The energy barrier of this reaction is calculated to be 17.5 kcal/mol (Table 3). This barrier is not markedly higher than that of $2 \rightarrow 1$ retro-cyclization, and this path might not be removed from the decomposition channels of **2**.

4. Summary

From the results of our theoretical investigation, we concluded that the singlet–triplet energy separation is quite similar in both *p*-benzyne and 1,4-diylnaphthalene. This is also true in **2** and **4**. Therefore, this is not the reason hydrogen abstraction is the rate-limiting step of a 10-membered cyclic enediyne **3**. The energy barriers for the retro-Bergman cyclization of the intermediates **2** and **4** are estimated to be 15.3 and 5.9 kcal/mol, respectively. The energy barriers of the hydrogen abstractions by **2** and **4** are roughly estimated to be 12.7 and 11.8 kcal/mol. These theoretical results indicate that the rate-limiting step along the Bergman reaction pathway of **3** is hydrogen abstraction rather than cyclization, while cyclization is the rate-limiting step along that of **1**. These results support the suggestions made by Kaneko et al.⁹

Acknowledgment. Financial support from a grant-in-aid for scientific research (no. 09554035) from the Ministry in Education, Science and Culture, Japan (to S.K.) is gratefully acknowledged.

Supporting Information Available: Table 1S contains Cartesian coordinates of all stationary structures. This material is available free of charge via the Internet at <http://pubs.acs.org>.

References and Notes

- Masamune, S., et al. *J. Chem. Soc., Chem. Commun.* **1971**, 1516.
- (a) Berman, R. G., et al. *J. Am. Chem. Soc.* **1972**, *94*, 660. (b) Bergman, R. G. *Acc. Chem. Res.* **1973**, *25*, 5. (c) Lockhart, T. P.; Commita, P. B.; Bergman, R. G. *J. Am. Chem. Soc.* **1981**, *103*, 4082.
- (a) Nicolaou, K. C.; Dai W.-M. *Angew. Chem.* **1991**, *103*, 1453. (b) Nicolaou, K. C.; Dai W.-M. *Angew. Chem., Int. Ed. Engl.* **1991**, *30*, 1387.
- Maier, M. E. *Synlett* **1995**, 13.
- Iida, K.; Hiram, M. *J. Am. Chem. Soc.* **1995**, *117*, 8875.
- Lhermitte, H.; Grierson, D. S. *Contemp. Org. Synth.* **1996**, *3*, 93.
- Grissom, J. W.; Gunawardena, G. U.; Klingberg, D.; Huang, D. *Tetrahedron* **1996**, *52*, 6453.
- Semmelhack, M. F.; Neu, T.; Foubelo, F. *J. Org. Chem.* **1994**, *59*, 5038.
- Kaneko, T.; Takahashi, M.; Hiram, M. *Tetrahedron Lett.* **1999**, *40*, 2015.
- (a) Ruedenberg, K.; Schmidt, M. W.; Dombek, M. M.; Elbert, S. T. *Chem. Phys.* **1982**, *71*, 41–49, 51–64, 65–78. (b) Schmidt, M. W.; Gordon, M. S. *Annu. Rev. Phys. Chem.* **1998**, *49*, 233–266.
- (a) Ditchfield, R.; Hehre, W. J.; Pople, J. A. *J. Chem. Phys.* **1971**, *54*, 724. (b) Hehre, W. J.; Ditchfield, R.; Pople, J. A. *J. Chem. Phys.* **1972**, *56*, 2257. (c) Hariharan, P. C.; Pople, J. A. *Theor. Chim. Acta* **1973**, *28*, 213. The d exponent used was 0.8 for C atoms, while 1.1 was used as the p exponent for H atoms.
- (a) Dunning, T. H. *J. Chem. Phys.* **1971**, *55*, 716. (b) 0.72 and 1.0 were used as the d exponent for C atoms and p exponent for H atoms, respectively.
- (a) Nakano, H. *J. Chem. Phys.* **1993**, *97*, 7983. (b) Nakano, H. *Chem. Phys. Lett.* **1993**, *207*, 372. (b) Exactly speaking, the method employed in this investigation is different from the so-called CASPT2.
- Schmidt, M. W.; Baldrige, K. K.; Boatz, J. A.; Elbert, S. T.; Gordon, M. S.; Jensen, J. H.; Koseki, S.; Matsunaga, N.; Nguyen, K. A.; Su, S.; Windus, T. L.; Dupuis, M.; Montgomery, J. A., Jr. *J. Comput. Chem.* **1993**, *14*, 1347–1363.
- Logan, C. F.; Chen, P. *J. Am. Chem. Soc.* **1996**, *118*, 2113. The energy barrier is estimated to be 9.5 kcal/mol for the hydrogen abstraction by **6** from methanol.
- Wierschke, S. G.; Nash, J. J.; Squires, R. R. *J. Am. Chem. Soc.* **1993**, *115*, 11958.
- Hoffner, J.; Schottelius, M. J.; Feichtinger, D.; Chen, P. *J. Am. Chem. Soc.* **1998**, *120*, 376.
- Schreiner, P. R. *J. Am. Chem. Soc.* **1998**, *120*, 4184.
- Squires, R. R.; Cramer, C. J. *J. Phys. Chem.* **1998**, *102*, 9072.
- Wenthold, P. G.; Squires, R. R.; Lineberger, W. C. *J. Am. Chem. Soc.* **1998**, *120*, 5279.
- Hoffmann, R.; Imamura, A.; Hehre, W. J. *J. Am. Chem. Soc.* **1968**, *90*, 1499.
- The Cartesian coordinates are available in **Table 1S** (Supporting Information).
- Since we have convergence problems of MCSCF iterations, we could not obtain MCSCF force constant matrices at the transition states. We only calculated GVB analytic force-constant matrices at the transition states, and these matrices were employed for MCSCF transition state searches. The transition state searches indicate that **TS** ($1 \rightarrow 2$), **TS** ($3 \rightarrow 4$), and **TS** ($2 \rightarrow 5$) are true transition states (only one imaginary frequency is generated).
- Kraka, E.; Cremer, D. *J. Am. Chem. Soc.* **1994**, *116*, 4929.
- Schottelius, M. J.; Chen, P. *J. Am. Chem. Soc.* **1996**, *118*, 4896. See also, the following: Chaban, G. M.; Gordon, M. S. *J. Phys. Chem. A* **1999**, *103*, 185.
- Roth, W. R.; Hopf, H.; Horn, C. *Chem. Ber.* **1994**, *127*, 1765.
- Deleted in proof.
- The MCSCF active space includes two radical σ orbitals in **2** and bonding and antibonding orbitals of a C–H in methane.
- Roth, W. R.; Hopf, H.; Wasser, T.; Zimmermann, H.; Werner, C. *Liebigs Ann.* **1996**, 1691.
- Hiram, M. Unpublished data.
- (a) Nicolaou, K. C.; Zuccarello, G.; Riemer, C.; Estevez, V. A.; Dai, W.-M. *J. Am. Chem. Soc.* **1992**, *114*, 7360. (b) Nicolaou, K. C.; Zuccarello, G.; Ogawa, Y.; Schweiger, E. J.; Kumazawa, T. *J. Am. Chem. Soc.* **1988**, *110*, 4866.
- (a) Nicolaou, K. C.; Dai, W.-M.; Hang, Y. P.; Tsay, S.-C.; Baldrige, K. K.; Siegel, J. S. *J. Am. Chem. Soc.* **1993**, *115*, 7944. (b) Nicolaou, K. C.; Hang, Y.-P.; Torisawa, Y.; Tsay, S.-C.; Dai, W.-M. *J. Am. Chem. Soc.* **1991**, *113*, 9878.